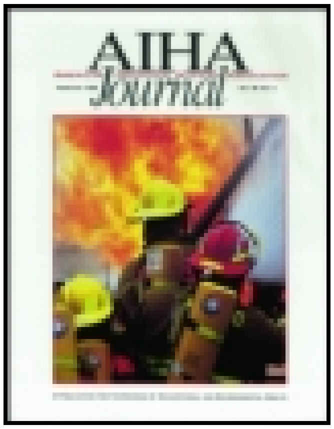

American Industrial Hygiene Association Journal
Publication details, including instructions for authors and subscription information:
http://www.tandfonline.com/loi/aiha20

Experimental Investigation of Power Loss Coefficients and Static Pressure Ratios in an Industrial Exhaust Ventilation System

Steven E. Guffey [a] & Jeffrey G. Spann [b]

[a] University of Washington, School of Public Health and Community Medicine, Department of Environmental Health, Box 357234, Seattle, WA 98195

[b] Washington Industry Safety and Health Administration, Washington Department of Labor and Industry

Published online: 04 Jun 2010.

Authors
Steven E. Guffey[a]
Jeffrey G. Spann[b]

[a]University of Washington, School of Public Health and Community Medicine, Department of Environmental Health, Box 357234, Seattle, WA 98195;
[b]Washington Industry Safety and Health Administration, Washington Department of Labor and Industry

Experimental Investigation of Power Loss Coefficients and Static Pressure Ratios in an Industrial Exhaust Ventilation System

A study tested whether measures of equivalent resistance (X values) and ratios of static pressure (SPratio) for given ducts of contaminant control exhaust ventilation systems were independent of substantial changes to airflow level and to changes to resistance of other ducts within the same full-scale five-branch system. In a factorial study design, four airflow levels were achieved by changing fan rotation rate while resistances to flow for specific branch ducts were changed independently by adjusting slidegate dampers to various settings. For each damper insertion depth (including fully open), the results demonstrated substantial invariance for branch X values (few greater than 5%), SPratio (few greater than 3%), and fraction of airflow to each duct (few greater than 2%). X-values for submains were much less stable, changing by 20% or more with changes to other parts of the system. For the same conditions, hood static pressures changed by as much as 96% (with standard deviation of 40%). The results suggest that before and after values of X and SPratios should be more reliable bases for indicating alterations than comparison of observed static pressures. The stability of airflow distributions with substantial changes in airflow suggests that one could adjust airflow distribution (e.g., with dampers) without considering whether the fan speed was set correctly, leaving fan adjustments for a final step.

Keywords: ventilation

For ventilation systems to control airborne contaminants reliably with the minimum total airflow (and costs), ventilation texts widely agree that it is imperative that they distribute the total airflow the fan provides among the hoods at specified levels.[1–7] However, in the experience of the authors industrial exhaust ventilation systems often do not provide the specified distribution of airflows to the hoods. The problem sometimes is a result of poor design. However, even a well-designed system can eventually provide a poor distribution of airflow as a result of mechanical damage, partial blockage of ducts by settled dust or sticky contaminants, incorrect damper adjustments, maintenance mistakes or omissions, or other forms of abuse or neglect. Attempts to discover the location of the problems (troubleshooting) by comparing before and after static pressures or airflows can be time-consuming and frustrating because a physical change in any part of the system changes airflows and pressures everywhere in the system.[8]

As aids to discovering the location of system alterations, a previous publication[9] identified two parameters for quantifying the physical status of individual ducts in vent systems: dissipated power coefficients (X) and static pressure ratios. The most convenient static pressures to employ for a static pressure ratio in a branch duct is the hood static pressure (SP_H) and the static pressure measured just upstream of the junction fitting at the end of the branch duct (SP_{br}). Values of X and SP_H/SP_{br} should remain nearly constant except when there has been a physical change in the duct under consideration; thus, comparisons of before and after values should help determine

Funding provided by the National Institute for Occupational Safety and Health in grant number 1 RO1 OH03165.

whether a change has occurred in a given section of the system ductwork.

If values of X are largely constant under fixed conditions, it also may be possible to use observed X values to model installed systems, providing a basis for predicting the effects of desired changes to the system,[8] including predictions necessary for a proposed airflow rebalancing method.[10]

DEFINITION OF X VALUES

As described in much greater detail elsewhere,[11,12] the dissipated power coefficient (X) for any contiguous section of duct is defined as difference in total energy rate entering and exiting that section (i.e., the dissipated power) divided by kinetic power:

$$X = \frac{\text{Power In} - \text{Power Out}}{KP} \quad (1)$$

where: KP = kinetic energy rate.

For steady-state flows, the total power of the flow at a cross section can be written as the integral sum of powers related to static pressure, internal energy, momentum change, and elevation potential over the area.[13–15] For the conditions of interest to industrial ventilation, the total power of the flow at a cross section can be computed at the cross section as a simple algebraic relationship:

$$\text{Power} = Q\ TP \quad (2)$$

where Q = airflow at the cross section, and TP = mean total pressure at the cross section.

The kinetic power of the flow can be computed from:

$$KP = Q\ VP \quad (3)$$

where VP = mean velocity pressure at the cross section.

If one limits the discussion to the converging flows found in an industrial exhaust system, there is only one exit flow from a section of duct. However, there are often up to three flows entering a junction fitting. Combining Equations 1, 2, and 3, values of X can be computed for converging flow systems from:

$$X = \frac{\sum_{i=1}^{n} Q_i TP_i - Q_{exit} TP_{exit}}{QVP} \quad (4)$$

where i = ith cross section for flow entering upstream; n = number of flows entering from upstream; and exit = cross section at end of the section of duct.

X can be calculated for any bounded volume in a ventilation system (i.e., a contiguous section of the duct system) from a single elbow or junction to an entire branch or subsystem of branches. When computing interactions with the fan, the entire system can be represented by a single value of X. Any section of interest for troubleshooting purposes can be singled out, as long as it is a continuous volume with all inlets and outlets known. For this study and for troubleshooting real systems, the two types of sections of greatest interest are branch ducts and submains (the duct connecting two junction fittings). Applying Equation 4 to a branch produces the familiar form of a velocity pressure loss coefficient since the upstream pressure is zero and the same airflow is in the numerator and denominator.

$$X_{end} = \frac{-TP_{end}}{VP_{end}} \quad (5a)$$

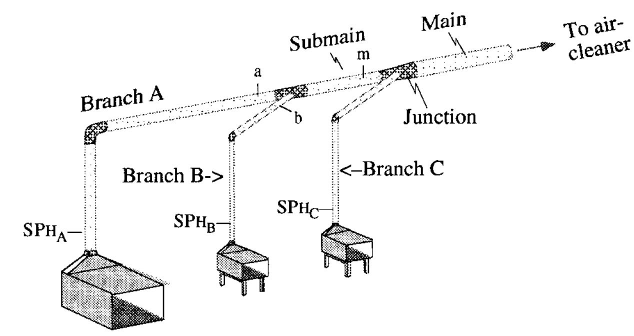

FIGURE 1. An example portion of a system

where end = cross section a few diameters length upstream of the junction fitting.

For example, the equivalent resistance for Branch A in Figure 1 (i.e., X_{br_a}) would be computed from the total pressure and velocity pressure at Cross Section a, which is chosen to be as near the junction fitting as possible without becoming so close that measurement conditions substantially reduce measurement accuracy (e.g., at least three duct diameters distance). If Branch A has the same cross-sectional area and shape for its entire length, X_{br_a} would be equivalent to the sum of velocity pressure coefficients for the portion of Branch A upstream of Cross Section a. Note that changes to the portion of the branch from a to the junction fitting are omitted by this definition.

Applying Equation 4 to other sections of a ventilation system can produce much less familiar forms. For example, for the volume in Figure 1 bounded by cross sections at a, b, and m, Equation 4 would be stated as:

$$X_{a\text{-}b\text{-}m} = \frac{Q_a TP_a + Q_b TP_b - Q_m TP_m}{Q_m VP_m} \quad (5b)$$

Note that Volume a-b-m includes not just the submain, but the junction fitting and the short sections from Cross Sections a and b to the junction fitting. Determining the value of X for the submain directly would be difficult since pressures measured just downstream of a junction fitting are likely to be highly inaccurate. Use of Equation 5b presents advantages and disadvantages. The advantage is that all portions of the system upstream of cross sections m are included when defining X_{br_a}, X_{br_b}, and $X_{a\text{-}b\text{-}m}$. The disadvantage is that $X_{a\text{-}b\text{-}m}$ would not be completely independent of conditions upstream of a and b since the airflow through the portions of the two branch ducts downstream of Cross Sections a and b, respectively, are not equal to Q_m. In addition, the equivalent resistance for flow through a junction fitting (X_J) has been show elsewhere to vary with the relative airflows through the upstream ducts.[10–12] Thus, one would expect that large changes in the relative velocities in Ducts a and b would produce changes in $X_{a\text{-}b\text{-}m}$ even when the submain had experienced no obstructions or other changes. The latter effect can be removed by estimating the contribution to junction fitting losses and subtracting it from $X_{a\text{-}b\text{-}m}$.

$$X_{sub} = X_{a\text{-}b\text{-}m} - \frac{k_a Q_a VP_a + k_b Q_b VP_b}{Q_m VP_m} \quad (6)$$

where ka, kb = empirical coefficients,[12] which are functions of junction geometry.

PROPERTIES USEFUL FOR TROUBLESHOOTING

For the high duct velocities (1500 to 6500 ft/min) that typify industrial exhaust systems,[1] the dissipated energy per time (i.e., Power in-Power out) varies nearly linearly with kinetic power,[11,12] so values of X should vary only slightly with changes in Q over a wide range of airflow (e.g., ±50%) and pressure changes.[9] Thus, a significant change from the baseline value of X for any part of a ventilation system should occur only if there has been a physical change in that section, and values of X could be used to pinpoint the location of changes in any section for which prior static pressure (SP) and velocity pressure (VP) measurements have been made.

Two other properties of X values are of interest in troubleshooting. First, changes in X can be compared directly with velocity pressure coefficients. Indeed, velocity pressure coefficients can be considered the subset of X values for individual components.[12] For example, a change in X value of 0.20 is equivalent to adding a component with the same velocity pressure coefficient (e.g., a typical elbow). Furthermore, for a duct with constant cross section and no junctions or leaks, the observed value of X should be equal to the sum of the velocity pressure coefficients for components (e.g., elbows, straight duct) in that length of duct. Thus, comparison of observed X values to expected sums of loss coefficients provides a means to evaluate newly installed systems independently of airflow level.

Second, changes in X are directly related to changes in airflow distribution. For example, for two ducts (see Figure 1) terminating at Cross Sections a and b, respectively, upstream of a junction fitting, the distribution of airflows between them (Q_a and Q_b) are governed by:[10]

$$\frac{Q_b}{Q_a} = \frac{A_b}{A_a}\sqrt{\frac{\rho_a}{\rho_b}}\sqrt{\frac{1 + X_a + Fen_a}{1 + X_b + Fen_b}} \quad (7)$$

where Fen_a, Fen_b = empirical velocity pressure coefficients for junction entry (used in power loss calculations); ρ = density of the airflow; and A = cross-sectional area.

Fena and Fenb have been shown[12] to be independent of airflow (Q), and, of course A_b and A_a remain constant unless the ducts are replaced. Thus, there can be no change in airflow distribution (Q_b/Q_a) without changes in X_a or X_b, and they change only if there has been a physical change in the ducts they characterize. It follows, therefore, that the ratio of each branch airflow to the total system airflow must remain constant unless there has been a modification to the system. Conversely, detection and removal of unwanted changes to the system should restore the original X values and the original airflow distribution.

An accurate determination of an X value requires a time-consuming velocity pressure traverse. It would be convenient if it were possible to detect substantial changes in X without performing a velocity pressure traverse. Ratios of static pressures may do just that. Clearly, the ratio of two X values between different points in a ventilation system should be constant unless there has been a physical change in the volumes containing either point. As has been derived elsewhere, the ratio of any values of X determined at any two locations in the same system should be proportional to the ratios of the static pressures measured at those locations.[9,10] For example, for the branch in Figure 2:

$$\frac{1 + X_H}{1 + X_{end}} = \frac{SP_H}{SP_{end}} \quad (8)$$

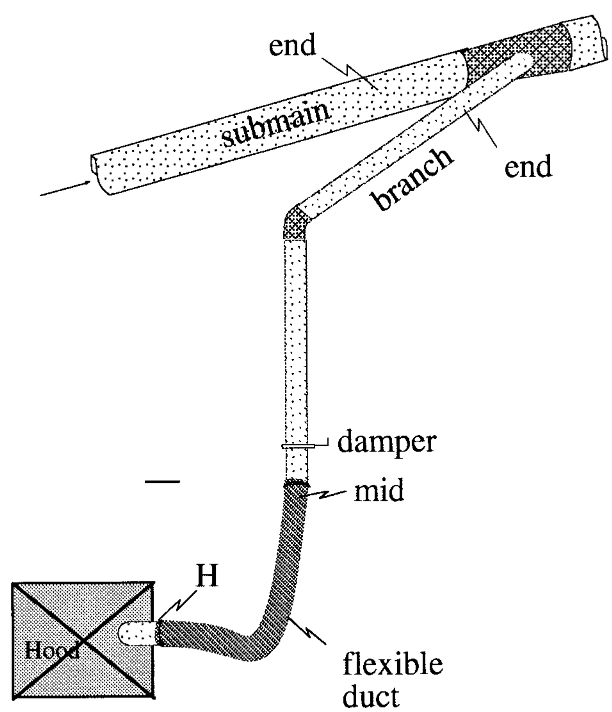

FIGURE 2. An example branch

Thus, change in SP_H/SP_{end} can be used as a surrogate for change in the value of X for a branch. The advantage of the static pressure ratio is that it does not require time-consuming velocity pressure traverses. The disadvantage compared with X values is the inability to relate changes in static pressure ratio directly to changes in airflow distribution.

Another useful property of these parameters is robustness with errors in determining density or instrument gain. For the narrow ranges of temperatures and barometric pressures in the study, all of the observed values (SP_H, SP_{end}, VP) should vary linearly with changes in density. Likewise, all of the pressure measurements would be proportional to the gain of the instrument whether the gain was set correctly or not. Since the numerator and denominator for both X and SP_H/SP_{end} are each proportional to the density[10] and the gain of the pressure sensor, the values of X and SP_H/SP_{end} should be unaffected by most errors in determining density or instrument gain. It is necessary only that the pressure device be stable during a round of measurements.

STUDY DESIGN

It would be convenient if power loss coefficients (X) and static pressure ratios varied only with modifications made within the set of ducts they define. If so, they could be highly certain indicators of whether a given duct has suffered alterations. It would be particularly useful if values of X were stable when dampers were used within branch ducts since their instability would adversely affect the accuracy of a proposed balancing method.[10]

To test the stability of X values and static pressure ratios, overall airflow levels and branch resistances to flow were varied in a full-scale, five-branch ventilation system. Data runs in this study involved three different mixes of damper settings. Damper Group 0 had all dampers open, providing a baseline condition. Damper

TABLE I. Ductwork Measurements

Duct	Type	Duct i.d. (inches)	Length[A] (feet)	No. of 90° Elbows[D]	Straight-Run Duct[B] Diameters	Distance from Traverse pt. to Junction[C] (inches)
1	branch	6.999	32	0[D]	51	27
2	branch	4.992	33	0.5[D]	31	24
3	branch	4.990	32	0.5[D]	31	24
4	branch	5.994	31	0.5[D]	26	26
5	branch	6.995	40	0.5[D]	55	93
10	submain	7.995	18	0	24	35
20	submain	9.969	18	0	18	39
30	submain	12.007	65	2[A]	32	70
40	submain	12	5	0.5[E]	n/a	n/a
W	expansion	12/17	3	0	n/a	n/a
X	main	17	2	0	n/a	n/a
Fan	fan					
Z	stack	17	21	2	n/a	n/a

[A]All submain elbows were five-section 90° turn (radius = 2 D).
[B]Distance between junction measurement point and nearest upstream obstruction (branch entry or elbow), in duct diameters.
[C]Distance between measurement point and center of junction.
[D]All branch elbows were stamped and turned 45° (radius = 1.5 D).
[E]Eight-section adjustable; approximately 45° total turn.

Group 1 had dampers partially closed for all but Branch B. Damper Group 2 also had dampers partially closed for all but Branch B, but the insertion depths were different from those of Group 1. For each damper setting group, total system airflow was adjusted to four levels by adjusting the bleed-in and the fan rotation rate.

The dependent variables were fraction of airflow for each branch, value of X for each branch or submain, and value of SP_H/SP_{end} for each branch. The independent variables were branch or submain identity, level of airflow at the fan, and damper insertion depth for each branch.

APPARATUS

The tested ventilation system and the measurement apparatus have been described in detail elsewhere[16,17] and will be described briefly here.

Ventilation System

The tested ventilation system was located at the University of Washington Department of Environmental Health Ventilation Lab. The system consisted of five branches, three submains, the main duct, and the exhaust fan (see Table I and Figure 3).

The ductwork was assembled from standard spiral-wound 20- and 22-gauge round galvanized steel duct. The duct system was constructed from 10-ft straight lengths (and shorter pieces where needed), elbows, junctions, expansions, and blastgate dampers. The hoods were unflanged duct-end inlets. Each branch had a slidegate damper (“blastgate”) located between 6 and 10 ft downstream from the duct entrance. The dampers were of leakproof construction. Ducts were connected with 4-inch long, 18-gauge galvanized steel insert couplers. The ductwork was supported at 6-ft intervals.

The straightness of each run of duct in the horizontal plane was verified by a taut string and level. For straightness in the vertical plane, the heights of supporting steel channel pieces were set originally with a rotating laser.

Air was drawn through the system by a centrifugal fan whose rotation rate was changed by substituting different pulleys on the motor output shaft. An electronic tachometer mounted on the fan shaft displayed the fan rotation rate to the nearest 1 rpm. The rotation rate during any given data run (4 to 8 hours) never varied by more than 1 rpm.

A “bleed-in,” consisting of 12 × 12 × 7-inch junction fitting installed in the main duct between the fan and the entry point of the most downstream branch (see Figure 3) was used to make fine adjustments in airflow through the system. With the air bleed open, less air flowed through the system branches, providing a different set of airflow conditions without changing the motor pulley.

Measurement Apparatus

Each branch and submain terminated upstream of a junction fitting in a section of drawn-over-mandrel (DOM) steel tube having the same inside diameter as the incoming galvanized duct (see Figure 4). Inside diameters at the downstream ends of these machined tubes were measured to the nearest 0.001 inch with a dial-reading caliper in three directions separated by 120°. The maximum variation in any tube was 0.023 inches.

To determine average flow velocity in each branch and submain, velocity pressures were measured using three pitot tubes mounted 120° apart at the same cross section (see Figure 4). Ten log-linear insertion depths were used for each traverse.

Static pressures were measured at centerline through the three pitot tubes at each DOM measurement station and through a bulkhead fitting in the duct wall four duct diameters downstream from each branch hood. Pressure was conducted to the manometers and electronic pressure transducer through clear plastic tubing (3/16-inch inside diameter, 1/16-inch wall thickness) connected with plastic quick-disconnect fittings. A plastic manifold and Luer-Lok® valve system allowed for quick changes from measurement by electronic transducer alone to concurrent measurement by transducer and inclined manometers without producing sudden changes to zero pressure.

Velocity pressures were measured with an electronic pressure transducer. Centerline velocity pressures were measured with both a transducer and an inclined manometer. Pressure applied to the transducer produced a proportional voltage, which was logged to

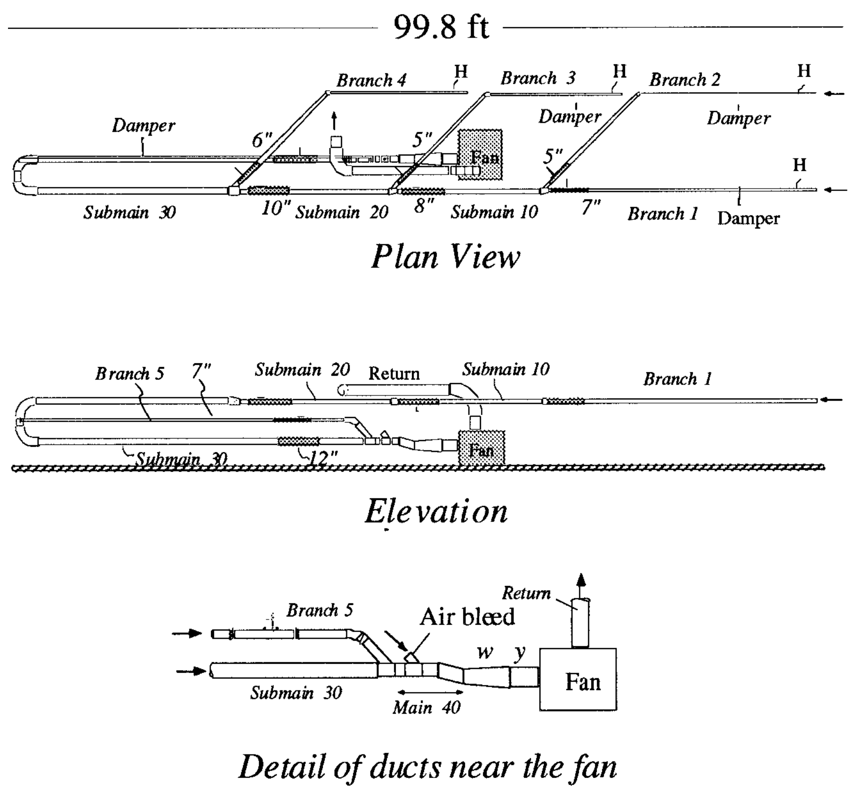

FIGURE 3. Ventilation system scale drawing

a computer file by an analog-to-digital converter. To check accuracy and correct for pressure-induced zero shift, the transducer was calibrated eight times during each data run against a 40-inch long, 4-inch w.g. inclined manometer marked in 0.01-inch intervals. An identical manometer was used for reading static pressures below 4-inch w.g. at measurement stations and duct entrances. Static pressures above 4-inch w.g. were measured with a 0–5.5 inch w.g. inclined manometer or a 0–16 inch vertical manometer.

Immediately before and after each data run, both the 4-inch w.g. manometers and the pressure transducer were calibrated against a Dwyer hook gage. Positive pressure for these calibrations were supplied by a small hand pump connected through the plastic static pressure manifold to all the measurement devices.

Barometric pressure was measured with a mercury barometer with a Vernier scale readable to the nearest 0.1 mm Hg. Readings were corrected for temperature and gravity according to the manufacturer's instructions. The barometer was calibrated by periodic comparison with readings provided by the nearest U.S. Weather Bureau station. Readings (corrected for elevation) never varied from those of the Weather Bureau by more than 1.5 mm Hg.

Duct temperatures were measured through a 3/8-inch hole in each duct at locations about one duct diameter length upstream from the DOM measurement station using a digital-readout thermometer with a resolution of 0.1°C. The digital thermometer was calibrated several times during each data run against a mercury thermometer traceable to the National Institute of Standards and Technology and readable to the nearest 0.1°C. The thermometer generally read 1.0°C. higher than the mercury thermometer; that amount was subtracted during data analysis.

Room dry and wet bulb temperatures were measured with a battery-powered psychrometer whose thermometer marked in 0.5°C divisions. The dry-bulb thermometer of the psychrometer typically read about 1.5°C higher than that of the mercury thermometer, and the dry reading of the wet-bulb thermometer was typically about 0.5°C higher than that of the dry-bulb thermometer. However, those errors were trivial in determining effects of water vapor on air density. Although environmental data were diligently recorded and the transducer was calibrated frequently, neither were particularly relevant since all readings would vary proportionately to both density and instrument gain.

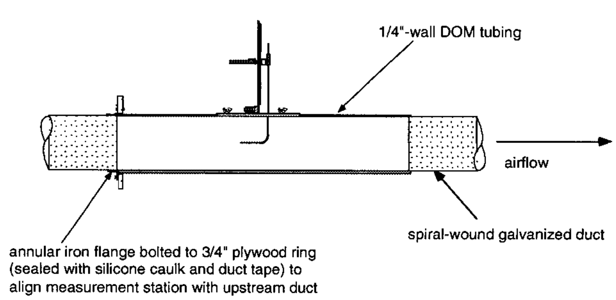

FIGURE 4. One of three pitot tubes in traverse device at measurement station

METHODS

Before any experiments were conducted the duct inlets were all capped and the fan left running while all leaks were found and

TABLE II. Damper Insertion Depths in Inches

	Branch				
	Br_1	Br_2	Br_3	Br_4	Br_5
Damper Setting Group 0	0	0	0	0	0
Damper Setting Group 1	3.12	0	2.00	1.25	3.21
Damper Setting Group 2	3.12	0	0.63	2.79	4.24

sealed. After the last experiment, the process was repeated. No leaks had developed. Before every test run, the digital thermometer was calibrated against a calibrated thermometer. Immediately before and after each data run, the transducer and inclined manometers were calibrated against a Dwyer hook gage using about 20 calibration points over the range of interest. Statistical regression of the transducer voltages and the hook gauge pressures produced a linear predictive equation used to compute pressures from transducer voltages. R-square values were typically 0.995 or better. To correct for transducer zero shift during measurements, three centerline velocity pressure readings (one from each pitot traverse) were made at each of the eight measurement stations using a 40-inch inclined manometer at the same time that the corresponding transducer voltages were logged.

For every test run, values of SP_{end} were measured at about three duct diameter's length (3D) upstream of the terminus of each duct. Values of hood static pressure (SP_H) were measured at about 3D downstream from the duct opening for each branch. For each branch, the three velocity pressure traverses were conducted at the DOM measurement stations and the duct temperature was measured just upstream of the DOM stations. Barometric pressure, wet bulb temperature, and dry bulb temperature were measured in the room.

During the experiments there were three combinations of insertion depths for the branch dampers, including a combination with dampers completely open (see Table II). In addition, there were four levels of fan airflow (Q_o, $1.15*Q_o$, $1.4*Q_o$, $1.6*Q_o$). Each damper combination was tested at each of the airflow levels. The "all dampers open" condition was tested again at the initial airflow level to provide a measure of measurement variability.

Data reduction of transducer voltages and environmental conditions to pressures and flows has been described in detail elsewhere,[17] and will be summarized briefly here. Pressures were computed from measured voltages and a first-order equation developed from linear regression of daily calibration data. The velocity at each pitot insertion in a traverse was computed from the velocity pressure for that insertion and the air density at that location. Density was computed using measured duct temperature, static pressure in the duct, barometric pressure, and humidity. The velocity contours for all traverses were inspected for missing data points and obvious errors (stepping on the plastic tubing during a measurement). Any remeasurements were done immediately.

The mean velocity was computed from the average of the 30 individual velocities. The mean velocity pressure was computed from the square of the average of the square roots of individual velocity pressures, which is mathematically identical to computing it from the density and the mean velocity.

As a test for leaks across junctions and as a general indication of the precision of airflow measurements, the sum of the measured upstream flows was compared with the flow measured in the submain downstream from each junction for all 13 data runs. For the junctions at the upstream ends of Submains 10 and 20, the mass balance differences are all within ±1.1% (mean = +.02%), indicating very small random measurement errors and no leakage. The

TABLE III. Percentage Deviations from Mean Values of SP_H, X, and SP_H/SP_{end} for Given Duct and Damper Settings

Parameter	Max. (%)	Std. Dev. (%)
For all branches, SPH_H[A]	96	40
For all branches, X_H[B]	8.6	3.3
For all branches, X_{br}[A]	6.2	2.5
For all branches, X_{sub}[B]	20	14
For all branches, SP_H/SP_{end}[A]	3.2	1.1

[A]Used different mean for each duct and damper setting.
[B]Used different mean for each duct but not for damper setting.

measurement point in Submain 30 was 65 feet downstream from the junction. The mean difference of −2.2% indicates some leakage in that length of duct. The random measurement errors were still very low; values for all but one run were between −1.5 and −3.5%.

Values of X_{br} and X_{sub} were computed using Equations 5a for branches and 6 for submains, respectively. For branches, the ratio SP_H/SP_{end} was computed. The airflow for each branch was computed using the measured duct diameter and the mean velocity computed above. Note that a density error due to incorrect measurements of the environment would have little or no effect on computations of static pressure ratios, X-values, or the fraction of total airflow going to each branch since those errors would affect the numerator and denominator equally. The same would be true for errors in determining the slope of the pressure-voltage equation for the transducer.

RESULTS AND DISCUSSION

As is detailed below, the results showed that values of X, SP_H/SP_{end}, and airflow distribution were highly stable for the conditions studied, varying very little except in cases where they were expected to vary.

Hood Static Pressures

As shown in Table III, values of SP_H varied greatly with changes in airflow, as one would expect. The largest deviation of SP_H from the mean value of SP_H for a given branch duct at a given damper insertion was 96%, and the coefficient of variation was 40%. Hence, under the conditions studied, comparison of before and after value of SP_H could mislead one to believe that an alteration had occurred at a given branch when, in fact, the changes in SP_H were due entirely to changes in other parts of the system.

Values of X_H for Branches

Since no alterations were made to branches upstream of the hood static pressure measurement location (H), values of X_H for a given branch should have remained constant as the damper insertion depth and fan airflow were changed. As shown in Table III, values of X_H varied relatively little. The greatest deviation from mean value was 8.6% and the standard deviation of deviations was 3.3%. This compares quite favorably with the volatility of SP_H values.

Branch Power Loss Coefficient Values (X_{br})

As expected, values of resistance for entire branches (X_{br}) varied with damper insertion depth (see Figure 5). For example, Branch E had three substantially different damper insertion depths (see Table II) and three different groups of corresponding X values.

As predicted, values of X_{br} for a given branch with a given

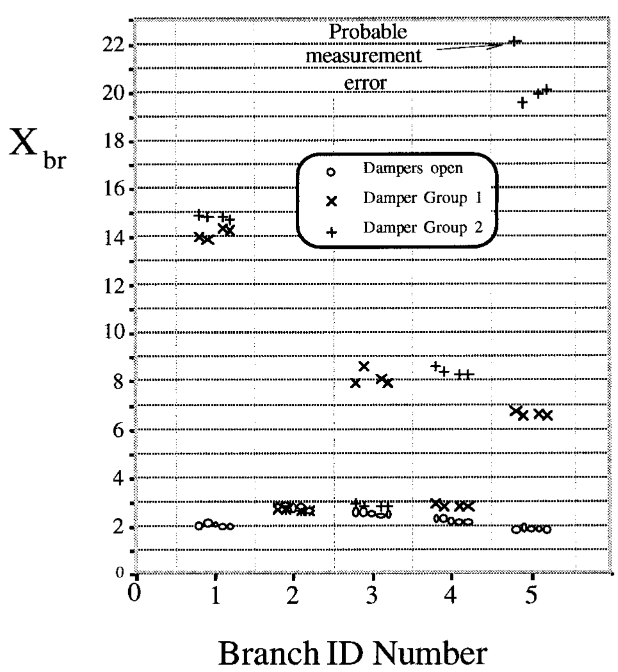

FIGURE 5. Values of X for each branch for each damper group

damper insertion depth (see Figure 5 and Table III) remained nearly constant as airflow rates were changed and as other branch dampers were adjusted. The maximum deviation of 6.2% was much greater than the second highest deviation (3%). The maximum may have represented a sampling or recording mistake. The coefficient of variation was only 1.5%. Note that the damper was wide open for all tests for Branch 2. As a result, the variability of X_{br} for Branch 1 was very low (<3%). On the other hand, the mean X values for Branch A differed somewhat for Group 1 and Group 2 even though the damper insertion depth for the two groups was the same (see Table II). It is possible that the group difference represents failure to return the damper to the same insertion depth.

As shown in Table III, the values of X_{br}, X_H, and SP_H/SP_{br} were relatively constant, showing coefficients of variation of 2.4, 3.5, and 0.7%, respectively. Of the 65 sets of branch X values (from 13 data runs in each of 5 branches), only 5 values showed greater than 4% deviations from the mean value at their damper settings. As shown in Table IV, values of X and SP_H/SP_{br} were not significantly associated with levels of airflow ($p>0.10$). Analysis involving nesting of Branch or Submain ID within other treatments had no effects on the conclusions, so the simpler analyses are presented here.

Damper Resistance (X_{damper}) and Insertion Depth

If X-values are to be useful, their values should increase with increasing obstruction to flow. In this study, a change in resistance for a branch could be due only to changes in the insertion depth of the damper, thus the contribution due to the damper (X_{damper})—the obstruction in this case—would be the X value for the branch

TABLE IV. Analysis of Variance

Source	df	Sum of Squares	Mean Squares	F-ratio	Probability
For X_{br} Using $\text{Log}(SP_{end}) - \text{Log}(VP)$					
Constant	1	33.8475	33.8475	534404	≤0.0001
Branch + Insertion/Dia.	11	4.83897	0.439906	6945.5	≤0.0001
Fan Speed and Bleed-in	1	0.001144	0.001144	18.070	≤0.0001
Error	51	0.003230	0.000063		
Total	63	4.93876			
For SP_H/SP_{end} Using $\text{Log}(SP_H) - \text{Log}(SP_{end})$					
Constant	1	10.5013	10.5013	389974	≤0.0001
Branch + Insertion/Dia.	11	4.63596	0.421451	15651	≤0.0001
Fan Speed and Bleed-in	1	0.000005	0.000005	0.179	0.6741
Error	51	0.001373	0.000027		
Total	63	4.74965			
For Submain Loss Coefficient (X_{sub})					
Constant	1	27.8301	27.8301	9760.8	≤0.0001
Fan Speed and Bleed-in	1	0.007772	0.007772	2.7258	0.1103
Damper Group	2	0.213827	0.106914	37.498	≤0.0001
Submain ID	2	0.605647	0.302823	106.21	≤0.0001
Damper Group*Submain ID	4	0.153996	0.038499	13.503	≤0.0001
Fan Speed and Bleed in*Submain ID	2	0.016769	0.008384	2.9406	0.0699
Error	27	0.076982	0.002851		
Total	38	10.0018			
For Q_{br}/Q_{fan} with Branch 5 excluded[A]					
Constant	1	1.75131	1.75131	8589.7	≤0.0001
Branch ID	3	0.045929	0.015310	75.089	≤0.0001
Fan Speed & Bleed-in	1	0.000174	0.000174	0.851	0.3616
Branch ID*Damper Group	6	0.056585	0.009431	46.256	≤0.0001
Error	41	0.008359	0.000204		
Total	51	0.116401			

[A]To avoid overfitting since sum of $\Sigma\, Q_{br}/Q_{fan} = 1$.

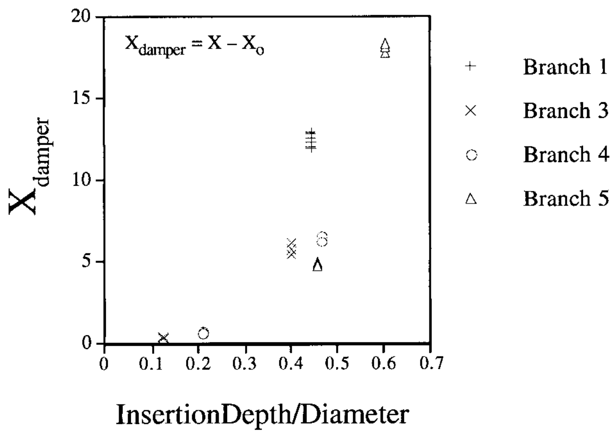

FIGURE 6. Change in resistance with damper insertion depth

with the damper partially inserted minus the value of X with the damper fully open (X_o):

$$X_{damper} = X - X_{damper} \quad (9)$$

One would expect the value of X for a branch to increase steadily as an increasingly large fraction of the duct was occluded. As shown in Figure 6, that is indeed what happened. The change in X value due to inserting a damper increased steadily as insertion depth increased. Note that the values of X_{damper} for the different dampers did not fall on a single smooth curve with increasing relative insertion depths, possibly due to the fact that the dampers were partially inserted to different depths even when the handle was pulled to its most open position.

Submain Power Loss Coefficient Values (X)

As shown in Table III and Figure 7, submain loss coefficient (X) values showed more sensitivity to modifications (i.e., lack of independence) to other parts of the system than did branch X values even though no physical changes were made within the submains themselves. However, large changes in submain power loss coefficients were observed only when the damper setting was changed in the branch joining the upstream end of the submain. Within each group of damper settings, variability in X for submains was greater than that for branches (see Table III).

Static Pressure Ratios

Branch static pressure ratio results are plotted in Figure 8. For a given damper setting, only 3 of the 65 data run branch static pressure ratios deviated by more than 2% from the mean value for that group. As shown in Table III, the most extreme deviation was 3.2%.

Airflow Balance

It would be convenient if airflow distribution varied only if the relative resistances to flow changed for branch ducts in the system. Since the test system had no hood filters or other components with nondynamic losses other than duct friction, one would expect its airflow distribution to change relatively little with overall airflow level. On the other hand, substantial changes in resistance due to changing damper insertion depths would be expected to change the airflow distribution.

As shown in Figure 9, the fraction of airflow through a given branch duct varied very little for a given group of damper insertion depths, despite changes to overall airflow level that reached nearly 70% for each damper group. Only one airflow in a branch deviated by more than 1% from the mean value for that damper setting for any of the tests—and it was only 2%.

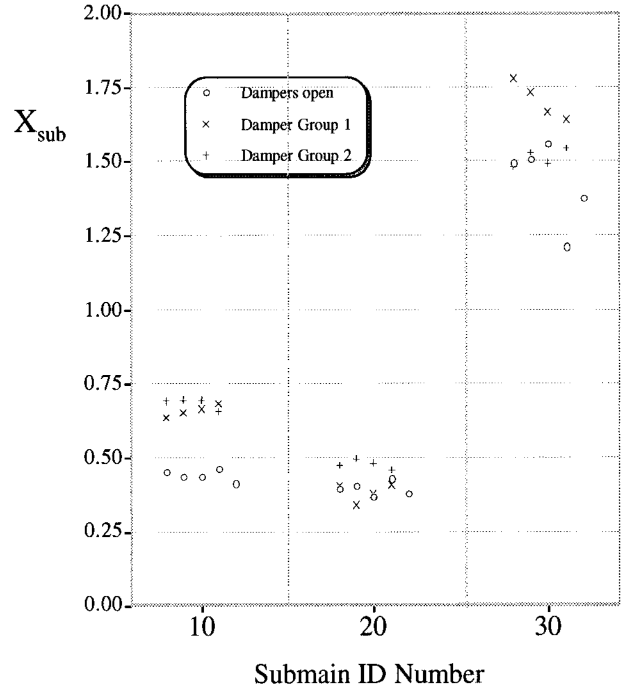

FIGURE 7. Submain X values for all damper groups and airflow levels

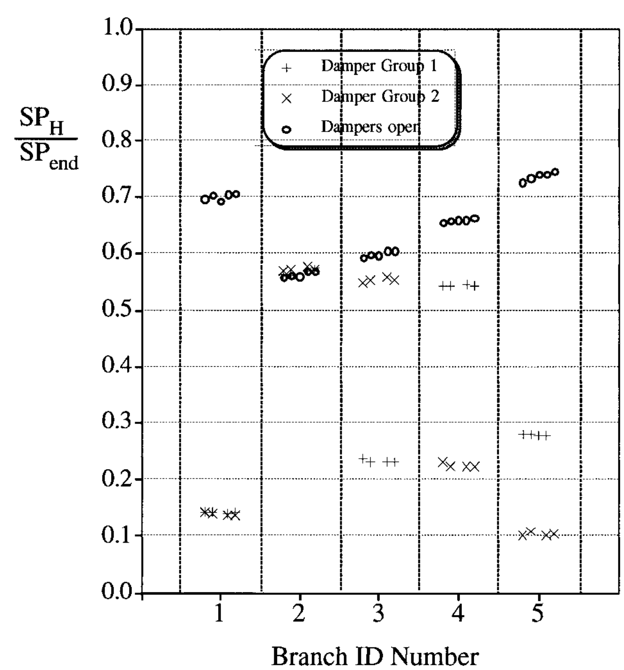

FIGURE 8. Static pressure ratios for each damper group at each of five airflow levels

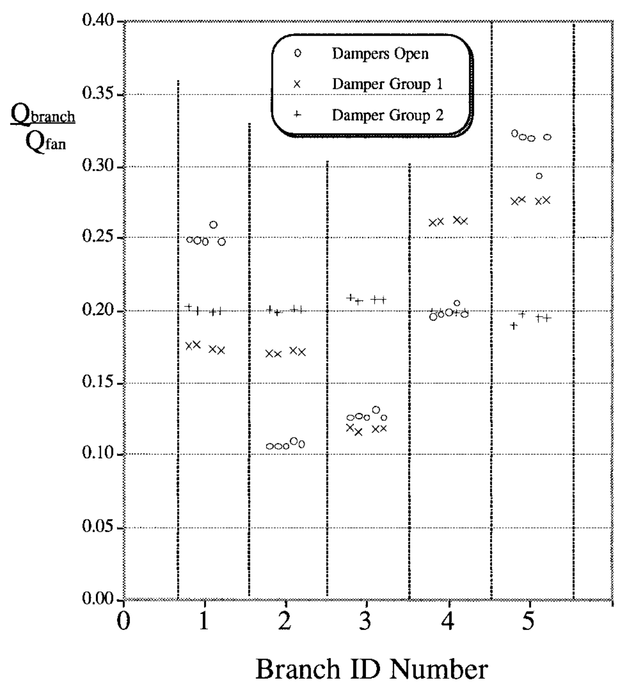

FIGURE 9. Distribution of system airflow among branches for each damper adjustment group at airflow levels

DISCUSSION

This study tested assumptions about the behavior of power loss coefficients (X), airflow distribution, and a static pressure ratio (i.e., SP_H/SP_{end}) as the system was modified or the fan speed was changed. For all branches and submains, it was expected that the values of X and SP_H/SP_{end} for a given branch would vary little from the mean value for a given damper setting as dampers were adjusted in other branches and changed the fan speed. Finally, a modification to one or more branches would alter the airflow distribution.

Compared with the values of SP_H, which varied with a standard deviation of 40%, the values of X_H, X_{br}, and SP_H/SP_{end} were relatively constant, showing coefficients of variation from their overall means of 3.3, 2.5, and 1.1%, respectively (see Table III). Of the 65 sets of branch X values (from 13 data runs in each of 5 branches), only 5 values showed greater than 4% deviations from the mean value at their damper settings.

Analyses of variance were performed to determine the sources of the variability of each dependent variable. For the dependent variables X_{br} and SP_H/SP_{end} the independent variables were surrogates for branch condition ("Branch+Insertion/Dia") and gross airflow level ("Fan Speed and Bleed-in"). Branch+Insertion/Dia is a variable contrived to separate different branch ducts and conditions from each other in the analyses. For example, Branch 1 should have different values of X_{br} and SP_H/SP_{end} than Branch 2. Furthermore, Branch 1 with a damper inserted to one insertion depth should have different values than Branch 1 with its damper inserted to a different insertion depth.

The deviations from the mean for values of X_{br} and SP_H/SP_{end} approached a normal distribution when log-transformed, so statistical analyses were performed on the log-transformed values. To test X_{br}, values of $\log[SP_{end}/VP]$ were analyzed since $\log[X_{br}]$ is the same as $10*\log[SP/VP]$. Note, also, that the log of a ratio is identical to the difference between the log of the numerator and the log of the denominator. That is, $\log[A/B]$ is the same as $\log[A]-\log[B]$. Thus, each of the dependent variables became the difference between the logs of two values determined by observation (e.g., VP, SP_H, and SP_{end}).

As shown in Table IV, values of X_{br} were significantly associated ($p<0.001$) with the variables controlling gross changes to fan airflow level (Fan Speed and Bleed-in). However, the contribution to the sum of squares was minuscule (less than 0.1%). As expected, Branch+Insertion/Dia was highly significant ($p<0.0001$) for both X_{br} and SP_H/SP_{end}. As expected and desired, branch condition almost completely accounted for the variability between cases.

As also shown in Table IV, values of SP_H/SP_{end} were independent of levels of airflow ($p>0.67$). As expected and desired, branch condition almost completely accounted for the variability between cases.

For the dependent variables X_{sub} and airflow distribution, the independent variables were ID, gross airflow level (Fan Speed and Bleed-in), and the combination of damper insertion depths (Damper Group). It was expected that X_{sub} would be independent of both independent variables and airflow distribution would vary with Damper Group, but not Fan Speed and Bleed-in.

The analysis of values of X_{sub} was quite different in methods and in results. Unlike X_{br} and SP_H/SP_{end}, X_{sub} is not computed from simple ratios, and log-transforming failed to improve the normality of the residuals. For those two reasons the untransformed values were analyzed. As shown on Table IV, values of X_{sub} were little affected by levels of airflow ($p>0.11$). However, where values of X_{sub} should have shown little association with damper group, they showed a strong correlation ($p<0.001$). This unwelcome association reduces the usefulness of X_{sub} in detecting and isolating obstructions in submains. However, if used with intelligence, X_{sub} could still be useful since large changes in X_{sub} occurred only when there had been a substantial physical change somewhere in the upstream ducts leading into the submain. An obstruction in the submain resistance could be recognized if values of X_{br} immediately upstream changed little. Conversely, a moderate change in X_{sub} should be discounted if accompanied by much larger changes in X_{br} immediately upstream.

Finally, one could hypothesized that airflow distribution would vary little for any given set of damper settings but not with changes in fan output. In fact, there was only one case (out of 65 branch runs) in which the fraction of total airflow deviated from the mean value for that group of damper settings by more than 1%. As shown in Table IV the fraction of system airflow passing through each branch was determined by the ID of the branch and the set of damper settings (Damper Group). Note that airflow distribution involves the relationship of each branch's airflow level to that of the total airflow through all branches. For that reason, the airflow through Branch 5 was excluded to recognize that loss of one degree of freedom. Omitting other branch ducts and including Branch 5 had negligible effect on the results. Residuals were non-normal, but transforming by logs, squares, and square roots did not substantially improve normality.

CONCLUSIONS

The results generally support the assumptions underlying the use of loss coefficient (X) and static pressure ratios (SP_H/SP_{end}) values for troubleshooting exhaust ventilation systems.

(1) Values of X and static pressure ratios for a branch were largely independent of airflow change in the branch, whether caused by

changes in overall system airflow (i.e., changing fan speed or bleed-in) or the adjustment of the damper in another branch.
(2) Values of X for a branch changed in a consistent manner when that branch's damper insertion depth was changed.
(3) Values of X for submains were less stable than values of X for hoods and entire branches. The values changed substantially when there was a modification substantially affecting the balance of airflow between the branches feeding the submain. Hence, changes to values of X_{sub} in the field should be interpreted cautiously.
(4) Airflow distribution ratios among the branches of the system remained constant for each damper group, an important finding since it suggests that one could adjust airflow distribution without first setting the fan speed to its optimal value, which is likely to be unknown until after the dampers are adjusted correctly.

Given their independence from airflow level and from modifications to other branches, values of X and static pressure ratios in branches could be reliable enough indicators of change to be useful as parameters for troubleshooting industrial exhaust ventilation systems. Detailed troubleshooting protocols using loss coefficients and static pressure ratios have been described elsewhere.[9]

The investigators noted that the dampers would not open fully, a common characteristic of slide-gate dampers. It would be useful if all dampers were manufactured so that the slides could be pulled to a fully open position without falling out of the gate.

It should be noted that the ventilation system employed in this study was far cleaner and its measurement conditions were far better than most industrial exhaust ventilation systems. Poor measurement conditions could produce much larger measurement errors, which in turn would inflate the apparent variability of values of X and static pressure ratios in the field. Thus, the optimal thresholds for action could be far higher than the 2–3% range of variability found here. An ongoing study seeks to determine the sensitivity and specificity associated with different thresholds for intervention in several working systems in industry.

REFERENCES

1. **American Conference of Governmental Industrial Hygienists (ACGIH) Committee on Industrial Ventilation:** *Industrial Ventilation: A Manual of Recommended Practice,* 23rd ed. Cincinnati, OH: ACGIH, 1997.
2. **American Society of Heating Refrigerating and Air-Conditioning Engineers:** *ASHRAE Handbook—1995 Fundamentals.* Atlanta, GA: ASHRAE, 1995.
3. **Brandt, A.D.:** Dividends from ventilation dollars. *Safety Engin.* (1950). pp. 14–15, 36–38.
4. **Alden, J., and J.M. Kane:** *Design of Industrial Ventilation Systems,* 5th ed. New York: Industrial Press, 1982.
5. **Baturin, V.V.:** *Fundamentals of Industrial Ventilation,* 3d ed. O.M. Blunn (trans.). New York: Pergamon, (1972).
6. **Burgess, W.A., M. Ellenbecker, and R. Treitman:** *Ventilation for Control of the Work Environment.* New York: John Wiley, 1989.
7. **Burton, D.J.:** *Industrial Ventilation: A Self-Study Companion to the ACGIH Ventilation Manual.* Salt Lake City, UT: Jeff Burton, 1982.
8. **Guffey, S.E.:** Modeling existing ventilation systems using measured values. *Am. Ind. Hyg. Assoc. J. 54*:293–306 (1993).
9. **Guffey, S.E.:** Quantitative troubleshooting of industrial exhaust ventilation systems. *Applied Occup. Environ. Hyg. 9*:267–280 (1994).
10. **Guffey, S.E.:** Airflow redistribution in exhaust ventilation systems using dampers and static pressure ratios. *Applied Occup. Environ. Hyg. 8*:168–177 (1993).
11. **Guffey, S.E., and D.A. Fraser:** A power balance model for converging and diverging flow junctions. *ASHRAE Trans. 95 (2)*:3–9 (1989).
12. **Guffey, S.E., and D.A. Fraser:** "Kinetic Power Model of Junctions Losses." Paper presented at ASHRAE National Summer Meeting, 1990.
13. **Ward-Smith, A.J.:** Internal fluid flow—the fluid dynamics of flow in pipes and ducts. Oxford, U.K.: Oxford University Press, 1980. pp. 25, 67, 69–71.
14. **White, F.M.:** *Fluid Mechanics.* 2nd ed. New York: McGraw-Hill. 1986. pp. 147, 167.
15. **Miller, D.S.:** *Internal Flow—A Guide to Losses in Pipe and Duct Systems.* Bedford, U.K.: British Hydromechanics Research Association, 1971.
16. **Guffey, S.E., and J.C. Curran:** Use of power balance to model pressures in bilateral junctions for converging flow ventilation systems. *Am. Ind. Hyg. Assoc. J. 54*:102–112 (1993).
17. **Guffey, S.E.:** A computerized data acquisition and reduction system for velocity traverses in a ventilation laboratory. *ASHRAE Trans. 98(1)*:98–106 (1992).